Alkaline sulphate fluids produced in a magmatic hydrothermal system – Savo, Solomon Islands

D. J. Smith [a, b]*, G. R. T. Jenkin [a], J. Naden [b], A. J. Boyce [c],

M. G. Petterson [a, b], T. Toba [d], W. G. Darling [e], H. Taylor [b], I. L. Millar [f]

[a] *Department of Geology, University of Leicester, LE1 7RH, UK*

[b] *British Geological Survey, Keyworth, Nottingham, NG12 5GG, UK*

[c] *Scottish Universities Environmental Research Centre, East Kilbride, Glasgow, G75 0QF, Scotland, UK*

[d] *Ministry of Mines and Energy, Honiara, Solomon Islands*

[e] *British Geological Survey, Maclean Building, Wallingford, OX10 8BB, UK*

[f] *NERC Isotope Geosciences Laboratory, Keyworth, Nottingham NG12 5GG, UK*

[*] *Corresponding author. Email dani1@bgs.ac.uk; Telephone +44 115 936 3100; Fax +44 115 936 3200*

Abstract

In magmatic-hydrothermal and associated geothermal systems, acidic magmatic-derived fluids (pH<3) commonly discharge from springs proximal to the vent of active (degassing) volcanoes and more alkaline (pH>5) geothermal fluids are typically limited to lateral outflows some distance from the main vent. Here we describe an unusual hydrothermal system associated with Savo volcano, a recently active (1830–40) trachyte-dominated island arc stratovolcano in the Solomon Islands. Hot springs (~100°C) near to the volcanic crater discharge alkaline waters instead of the more commonly recognised acidic fluids.

The hydrothermal system of Savo dominantly discharges sinter and travertine-forming alkaline sulphate (pH 7–8) waters at hot springs on its upper flanks, in addition to a small number of lower discharge acid sulphate springs (pH 2–7). Alkaline sulphate springs discharge dilute, chloride-poor (<50 mg/l), sulphate- (>600 mg/l) and silica-rich (>250 mg/l) fluids. They have restricted $\delta^{34}S_{SO4}$ (5.4 ± 1.5‰) and $\delta^{18}O_{H2O}$ values (−4‰; local non-thermal groundwater is −8‰). Acid sulphate springs discharge low chloride (<20 mg/l), high sulphate (300–800 mg/l) waters, with variable silica (100–300 mg/l) and distinctly lower $\delta^{34}S_{SO4}$ values (−0.6 ± 2.5‰) compared to the alkaline sulphate fluids. They also display high $\delta^{18}O_{H2O}$ and δD_{H2O} relative to non-thermal groundwater.

Geochemical modelling shows that water–rock reaction and dilution in the presence of secondary anhydrite, pyrite and quartz leads to chloride being diluted to low concentrations, whilst maintaining high sulphate and silica concentrations in the fluid. Strontium, oxygen and hydrogen isotopes confirm water–rock reaction and mixing with groundwater as primary controls on the composition of the alkaline sulphate springs.

The highly unusual dilute chemistry of all discharges at Savo is a consequence of high regional rainfall, i.e. climatic control, and results from open system mixing at depth between hydrothermal and meteoric waters.

1 Introduction

Studies of active magmatic-hydrothermal systems (e.g. Delmelle et al., 2000; Giggenbach et al., 2003) typically identify acid fluids discharging from springs in close proximity to the centre of hydrothermal activity. Fluids of higher pH in stratovolcano-hosted systems (near-neutral chloride type; Ellis and Mahon, 1977) are discharged as lateral outflows some considerable distance from the centre of activity (Henley and Ellis, 1983). However, near-crater (<1 km) hot springs on Savo, Solomon Islands, discharge high pH (7–8) sulphate-rich,

low-chloride fluids which precipitate silica sinter and mixed silica–carbonate deposits. Although acid springs do occur, the alkaline springs dominate in terms of number, discharge rate and longevity. The abundance of alkaline springs in an environment that might reasonably be expected to be dominated by acidic fluids (either as volcanic condensate discharges, or steam-heated springs) is highly unusual, as is the low-chloride content of the fluids.

Here we present chemical and stable isotope analyses of fluids from the Savo hydrothermal system, and undertake geochemical modelling to examine the sources and history of the fluids, and elucidate the importance of processes such as water-rock reaction and fluid mixing in generating these anomalous alkaline sulphate fluids.

2 Background

2.1 Geology and Tectonic Setting of Savo

The Solomon Islands were formed by the ongoing convergence of the Indo-Australian and Pacific plates (Fig. 1). Southward subduction of the Pacific plate at the North Solomon Trench System commenced in the Eocene, and continued until the thickened lithosphere of the Ontong Java Plateau eventually "choked" the trench, resulting in a change of subduction polarity (Petterson et al., 1999). Northward subduction of the Indo-Australian Plate at the South Solomon Trench System began at around 6 Ma (Phinney et al., 2004). Partial melting of young oceanic crust of the Indo-Australian Plate beneath the Solomon Arc exerts a strong control on erupted magma chemistry (Johnson et al., 1987; König et al., 2007). Metasomatic enrichment of the mantle wedge by the stalled Pacific slab has been suggested to be an important control on the composition of magmas in Papua New Guinea (McInnes et al., 2001; Müller et al., 2001; Richards et al., 1990), and may also be significant for magma generation in the Solomon Islands.

Savo (Fig. 1), 35 km northwest of the Solomon Islands capital Honiara, is a dormant stratovolcano. It rises approximately 1500 m from the seafloor, with the upper 485 m emergent above sea level. The centre of the island is marked by a 1.5 km diameter crater. Historical Merapi-type eruptions have been recorded in 1568, 1830–40, and inferred at 1630–1670 AD (Grover, 1958; Petterson et al., 2003), forming volcaniclastic deposits (block-and-ash-flow deposits and fluvially reworked equivalents), with lava domes in the crater and south of the island, subsequently heavily vegetated. Erupted rock compositions are dominated by silica-saturated (hypersthene to quartz-normative) sodic trachytes (plagioclase + hornblende + biotite + magnetite; silica-saturated, quartz-absent) and mugearites (plagioclase + clinopyroxene + magnetite ± hornblende ± olivine; Smith et al., 2009).

2.2 Major Thermal Areas of Savo

Hot springs (60–100°C) and steaming ground occur on the upper flanks of the volcano (Fig. 1). The crater has no hot springs, but fumaroles (<120°C) and steaming ground are present. Thermal areas have a strong odour of H_2S, and native sulphur precipitates at higher temperature steam and gas outlets. Inland cold springs (<30°C) are rare on Savo. Most groundwater-recharged wells in the coastal villages are noticeably warm, between 30–40°C. Most springs are hosted in poorly consolidated volcaniclastic deposits. To investigate the hydrothermal system at Savo, two field campaigns (April–May 2005; September–October 2006) were carried out.

2.2.1 Eastern Springs – Rembokola

An approximately 10 m^2 area of boiling pH 7–8 springs occurs in the upper reaches of the Rembokola stream (Fig. 1), on relatively flat ground within the steep-sided valley approximately 1 km from the crater rim. The springs are small pools (<0.5 m diameter) emptying via small channels into the main stream channel. Spring flow rates vary over

timescales of a few minutes, and individual springs discharge at rates of less than1 kg/s. The Rembokola stream is dominated by thermal water contributions in the upstream part of the catchment resulting in water temperatures up to 80°C. Combined discharge from the springs was approximately 10–50 kg/s (susceptible to variations in rainfall and spring flow rate). White siliceous sinter forms a crust over much of the streambed and sediments adjacent to the hot springs.

2.2.2 Crater Wall Springs – Poghorovorughala

The Crater Wall is the largest and most vigorous of the hydrothermal areas, with springs, spouters and fumaroles. It is in the upper reaches of the Poghorovorughala stream (Fig. 1), in the south of the island. The area extends approximately 200 m along the steep-sided valley from the crater rim, with less than 30 m lateral extent from the stream.

There is extensive fumarolic ground at the Crater Wall area, particularly on the northern side of the stream valley. This is marked by kaolinite and abundant native sulphur at the surface and black pyrite-bearing mud beneath. Boiling alkaline hot springs (pH 7–8) are common, both pools within small depressions and as spouters on the valley wall, and in the stream bed (marked by bubbling and boiling water as they discharge into the stream). There are a small number of mud pots, and some small spouters. Many of the springs produce unusual carbonate + opal-A + anhydrite deposits, as both layered and rounded (lobate) structures surrounding springs and spouters. Many of the springs identified in 2005 were still active in 2006, although some had deposited sufficient travertine to block the conduits, thus greatly reducing discharge. For unblocked springs, discharge rates were similar to those of the Eastern area, estimated to be 0.1–1 kg/s. The combined discharge of the springs is similar to that of the Eastern area (10–50 kg/s).

Acid hot springs also occur in the Crater Wall area, but in contrast to the alkaline sulphate springs, the acid hot springs are destructive, and lie within cavities. These springs typically have very low water discharges (on the order of 0.001–0.010 kg/s) although vigorous bubbling indicates significant gas discharge rates. These springs were not persistent features over the two sampling periods.

2.2.3 Reoka

The Reoka hydrothermal field is an area (approximately 50 m^2) of hot springs and fumaroles on the flat ground in the lower reaches of the Reoka stream (Fig. 1). Ground and hot spring temperatures are typically 100°C. At the surface, advanced argillic alteration (kaolinite with minor alunite) is widespread, with grey pyrite-bearing mud found up to 30 cm below. In 2005, acid hot springs (pH 2–5) occurred as pools within depressions within the thermal area. The springs were isolated from the stream, and had very low discharge rates (<0.010 kg/s). Landslides occurred in 2006, burying large portions of the area including a number of springs and the original stream channel. In 2006, the springs in the Reoka area flowed into the stream (unlike in 2005), although during rainfall, the stream overflowed into the spring depressions.

2.2.4 Tanginakulu

Tanginakulu is a warm stream (28–35°C) fed by small, low discharge springs (~0.001 kg/s) at 45–50°C. Travertine deposits occur for much of the stream's length, and range from thin veneers cementing clasts on the stream bed, to >10 cm thick beds of travertine. No high temperature thermal areas occur within the Tanginakulu catchment.

3 Sampling and Analytical Methods

3.1 Water Chemistry

Water samples were collected directly from springs and from large containers of freshly collected well water. The water was pumped through a <0.45 μm in-line PTFE syringe filter using silicone tubing and a hand vacuum pump. To ensure all equipment was free from contamination by previous samples, approximately 150 ml of sample water was pumped and discarded three times before collecting the actual sample. pH was determined in the field from filtered and cooled (~50°C) samples using digital pH meters with automatic temperature compensation (Hanna Instruments HI98128 and 991001). For hot springs, pH was corrected to spring temperature (pH_C) using SOLVEQ (Reed, 1982; Reed and Spycher, 1984), by inputting measured fluid compositions (using estimated HCO_3^- contents where necessary) and re-equilibrating to the higher discharge temperature. No gas analysis was available to recombine into the water. Corrections are small, generally resulting in changes of <0.2 pH units. Additionally, a small number of pH measurements were made in situ – there was no appreciable pH difference between the in situ pH measurements and the pH_C values.

Dissolved inorganic carbon (DIC) content was determined in the field on filtered samples by titration; pH was adjusted to 8.3 by addition of NaOH, then titrated to pH 3.8 using a Hach® Digital Titrator with sulphuric acid to determine the volume of acid required to convert all dissolved bicarbonate to CO_2. Titrations were repeated until three results within 5% were obtained. Purging of CO_2 and back titration was not possible. Results were corrected for interference from SiO_2 and B, following Arnórsson (2000). Bisulphide (HS^-) analysis was not performed, and this species may provide interference for the titration, resulting in slight over-estimation of total carbonate for alkaline fluids. Results are expressed as mg/l HCO_3^- equivalent, although for acidic fluids (pH <3.8) values likely represent dissolved CO_2.

For each sample, an unacidified fraction for anion determination was decanted into a 28 ml HDPE bottle. A fraction for cation determination was collected in a 28 ml HDPE bottle and acidified by addition of 0.3 ml Tracepur® 69% HNO_3 (samples SV197–SV213 acidified with 1 ml).

All laboratory-based analyses were carried out at the British Geological Survey at Keyworth, UK, a UKAS accredited laboratory that participates in the Aquacheck proficiency testing scheme. Analyses conform to ISO 17025.

Major and trace elements, including total sulphur, were determined using a Fisons/ARL3580 ICP-AES with Gilson 222 Autosampler, using procedures described in Ault et al. (1999). Samples for ICP-AES were diluted by fivefold (2005) or twofold (2006) using 1% Aristar® grade HNO_3 to avoid solids precipitating in the nebuliser. A subset of trace elements was analysed by VG Elemental PQ ExCell quadrupole ICP-MS for 2006 samples using procedures outlined in Cook et al. (2002). Accuracy and precision were determined from repeat analysis of quality control solutions over a period of 12 months, and are summarised in the supplementary data. Detection limits differ between instruments and samples due to different dilutions, and are summarised in the results tables where appropriate.

Anions were determined using a Dionex DX-600 Ion Chromatograph system with ED50A Electrochemical Detector and AD20 Absorbance Detector modules, using procedures outlined in Charlton et al. (2003). Precision of IC data (based on long term quality control solution data, with >500 analyses) is F^- =3%; Cl^- =5%; NO_2^- =3%; NO_3^- =4%; Br^- =2%; and HPO_4^- =4%. Accuracy (difference between mean and target value) determined from the Aquacheck proficiency testing scheme was 0.8% for F^-, 0.6% for NO_2^-, 0.4% for Br^-, 0.3% for HPO_4^-, −1.3% for NO_3^-, and 3% for Cl^-.

Comparison of SO_4^{2-} as determined by ICP-AES (as total sulphur; SO_4^{2-} should be the dominant species in acidified samples) and IC showed significant discrepancy between the two techniques, particularly for 2006 hot springs, with SO_4^{2-} concentrations lower when determined by IC. Sulphate content was also measured by gravimetry of barium sulphate precipitated from acidified samples in the field (see Section 3.2). Sulphate contents determined by gravimetry were similar to ICP-AES data, rather than IC data, suggesting that the sulphate in the latter (unacidifed) samples had been subject to modification, either by bacterial reduction or mineral precipitation. Logistical constraints meant that time between sampling and analysis was over one month. Consequently, ICP-AES data for SO_4^{2-} are used in preference to results obtained by IC.

Charge balance error (CBE) was calculated for major species (H^+, Al^{3+}, Fe^{2+}, Ca^{2+}, K^+, Mg^{2+}, Mn^{2+}, Na^+, SO_4^{2-}, Cl^-, HCO_3^-). Total carbonate is presented as HCO_3^- equivalent, and is calculated as a monovalent anionic species for the purposes of charge balance. High CBE may occur due to inappropriate choice of valency for carbonate species (i.e. if carbonate species are dominated by CO_3^{2-}, rather than HCO_3^-). Charge balance error is higher for 2005 samples as no carbonate analyses were made. For samples where all major species have been included, CBE should ideally be within ±5%.

3.2 Sulphur Isotopes

For aqueous sulphate analysis, 75 ml (100 ml for 2006 samples) of filtered sample was decanted in the field into a HDPE bottle, acidified with 1 ml Tracepur® 69% HNO_3, and an excess of 5% $BaCl_2$ solution was added slowly to precipitate $BaSO_4$. In the laboratory, precipitated $BaSO_4$ was separated from the water by centrifuge, rinsed with deionised water, dried at 80°C overnight, and weighed to determine SO_4^{2-} concentration. These data were

compared with the ICP-AES results as an approximate measure of recovery; recoveries were 100% ± 10% with the exception of SV212 (80%).

Native sulphur crystals were picked by hand from altered rocks collected at fumarolic areas, washed in deionised water in an ultrasonic bath for five minutes and dried in a desiccator overnight.

Sulphur and sulphates were converted to SO_2 for mass spectrometry at the Scottish Universities Environmental Research Centre (SUERC) by conventional combustion procedures (Coleman and Moore, 1978; Robinson and Kusakabe, 1975). The sulphur isotope composition of the purified SO_2 was measured using a VG SIRA II gas mass spectrometer and standard corrections applied to raw $\delta^{66}SO_2$ values to produce true $\delta^{34}S$ relative to Vienna Cañon Diablo Troilite (V-CDT). Reproducibility and accuracy were monitored through replicate measurements of international standards NBS 123 (17.7 ± 0.3‰, n = 16), IAEA S3 (−31.6 ± 0.3‰, n = 16), NBS 127 (21.2 ± 0.8‰, n = 17) and SUERC's internal laboratory standard CP-1 (−4.6 ± 0.7‰, n = 24); mean values for standards are within error of the accepted values (Coplen et al., 2002; Lipfert et al., 2007).

3.3 Oxygen and Hydrogen Isotopes

In the field, a filtered, unacidified fraction for isotopic analysis was decanted into a 14 ml glass McCartney bottle with a rubber-lined cap. Oxygen isotope ratios were analysed at SUERC using an automated CO_2 equilibration technique (after Epstein and Mayeda, 1953) using 1 ml of sample and analysing the resulting equilibrated CO_2 on an Analytical Precision AP2003 continuous-flow isotope ratio mass spectrometer. Water was reduced to H_2 using a chromium furnace (Donnelly et al., 2001); this was analysed using a VG SIRA 9 mass spectrometer (2005 samples) and a VG Optima (2006 samples). Oxygen and hydrogen

isotopes were measured relative to V-SMOW. Reproducibility was within ± 1.0‰ for $\delta^{18}O$ and typically better than ± 5‰ for δD for natural samples.

The $\delta^{18}O$ of sulphate was measured at SUERC using the technique of Hall et al. (1991). Barium sulphate (recovered as in Section 3.2) was mixed with pure carbon in a platinum crucible and heated in a vacuum line to produce CO_2. Any CO produced was converted to C and CO_2 in a Pt-electrode vessel. The resulting CO_2 was analysed on a VG Isogas SIRA 10 mass spectrometer. Precision and accuracy were monitored by repeat analysis of international standard NBS 127 (8.6 ± 0.4‰, n = 10, accepted value 8.7‰; Kornexl et al. 1999).

3.4 Strontium Isotopes

Sr analysis was performed on unacidified water fractions at the NERC Isotope Geosciences Laboratories (NIGL). Sr was separated using standard techniques using Dowex AG50W-X8 ion exchange resin (Royse et al., 1998). Samples were loaded onto single Re filaments using a TaO activator, and analysed using a Thermo-Finnigan Triton mass spectrometer in static multicollection mode. The Sr blank at the time of analysis was 111 pg. Replicate analyses of the SRM987 standard solution gave an average value of 0.710263 ± 4 (1σ, n=50). Data are reported normalised to SRM987 = 0.710250.

4 Results

Hot spring discharges (T >80°C) are commonly classified according to dominant anion composition and pH, leading to four main categories: alkaline (or near neutral) chloride, acid sulphate, acid sulphate–chloride (or “volcanic waters”; Giggenbach, 1997), bicarbonate, and mixtures thereof (Ellis and Mahon, 1977). Hot springs from Savo are sulphate dominated, with some bicarbonate–sulphate springs (Fig. 2). However, the dominant alkaline sulphate springs on Savo do not fit into the classical categories. There are two types of sulphate-rich

hot springs at Savo, alkaline and acidic, which can be defined on the basis of chemistry, stable isotope ratios and physical nature of the spring.

4.1 Alkaline Sulphate Hot Springs

Hot springs defined as alkaline sulphate type are pH_C 7–8 and have a restricted $\delta^{34}S_{SO4}$ of 5.4 ± 1.5‰ (Table 1; Table 2; Fig. 3) and $\delta^{18}O_{H2O}$ values only slightly greater than local non-thermal groundwater. Sulphate $\delta^{18}O$ values for alkaline hot springs vary between 4.0 and 7.9‰.

Crater Wall springs (Table 1) are sulphate-rich (600–680 mg/l), with very low chloride (~5 mg/l) and moderate DIC (~90 mg/l HCO_3^- equivalent) and SiO_2 (~250 mg/l). Calcium is as high as ~250 mg/l, Na ~90 mg/l, K ~17 mg/l, and Mg ~12 mg/l. Only trace iron and aluminium are present (<0.05 µg/l). Important trace elements include Li (300 µg/l), Rb (60 µg/l), and Sr (3 mg/l). In general, the analysed springs contain total dissolved solids (TDS) of <2000 mg/l.

The Eastern Springs (Table 2) have similar sulphate contents to the Crater Wall springs (610–650 mg/l), but higher chloride (~40 mg/l; still remarkably low), lower DIC (~40 mg/l HCO_3^- eqv.) and higher SiO_2 (~375 mg/l). Sodium and potassium concentrations are higher (~200 and 28 mg/l respectively), and Ca and Mg lower (~100 and 5–10 mg/l respectively) than the Crater Wall springs. Trace element concentrations are low overall, with increased alkali metals (Rb ~120 µg/l, Cs ~50 µg/l) relative to the Crater Wall Springs. Arsenic contents are measurable at the Eastern Springs, with samples containing ~50 µg/l.

Fig. 4 shows oxygen and hydrogen isotope compositions of alkaline sulphate spring water. Alkaline sulphate hot springs are clustered at $\delta^{18}O = -4 \pm 0.8$‰ and $\delta D = -36 \pm 3$‰, with two outliers both showing enrichment of the heavier isotopes. SV208 shows considerable

enrichment of both ^{18}O and D, and also has the lowest $\delta^{34}S_{SO4}$ value (+3.8‰) of the alkaline sulphate springs.

4.2 Acid Sulphate Hot Springs

Springs classified as acid sulphate type have a distinct $\delta^{34}S_{SO4}$ of −0.6 ± 2.5‰ (Fig. 3), contrasting markedly with alkaline sulphate springs. They also display high $\delta^{18}O_{H2O}$ and δD_{H2O} relative to non-thermal groundwater, and pH_C <7 and often <4. A number of springs are connected to streams (particularly in the Reoka area) – these springs tend to have higher pH than isolated variants, but are classified as acid sulphate due to their physical appearance (alteration of surrounding regolith to a base-depleted assemblage of kaolinite + silica ± anhydrite ± alunite, as determined by XRD), cation chemistry and stable isotope composition.

The Crater Wall acid springs (Table 3) are low pH (<4) with high but variable sulphate (480–820 mg/l), SiO_2 ~300 mg/l, and low chloride (<6 mg/l). Alkali metals are very similar between acid sulphate and alkaline sulphate springs in Crater Wall, whereas the alkaline earths tend to have slightly lower concentrations in the acid springs (Sr <2 mg/l, Ca <200 mg/l). Iron and aluminium concentrations are three orders of magnitude higher in the acid springs. Acid springs in Reoka show similar chemical trends. Concentrations of alkali metals and alkali earths vary between locations. DIC correlates positively with pH, whereas Al and Fe show a negative correlation as anticipated.

The stable isotope composition of water ranges from $\delta^{18}O$ = −0.9‰ and δD = −27‰ to $\delta^{18}O$ = +6.8‰ and δD = −3‰. The data form a linear array with slope 2.9 (scatter around line is ±5.4‰ δD for 1σ). The two alkaline sulphate outliers also lie on this trend (Fig. 4). Sulphate $\delta^{18}O$ ranges from 1.3 to 5.2‰.

4.3 Bicarbonate–Sulphate and Cold Springs

A third class of hot spring on Savo has a more bicarbonate-rich chemistry (>200 mg/l HCO_3^- eqv.), with sulphate ~300 mg/l (Table 4). The bicarbonate–sulphate springs are lower temperature than the acid and alkaline sulphate springs (~50°C), with pH 6–7. $\delta^{34}S_{SO4}$ averages 5.4‰ which is identical to alkaline sulphate springs (Fig. 3), but isotopes of O and H are less enriched, and overlap with non-thermal ground water from Savo. Bicarbonate–sulphate springs are often associated with travertine deposits. For bicarbonate–sulphate spring SV422, major cations are dominated by Ca (200 mg/l) and Mg (98 mg/l), with lower Na (48 mg/l) and K (6 mg/l) than the alkaline sulphate springs. Only one analysis is presented here, but based on field measurements of pH, temperature and observation of travertine deposits, bicarbonate-sulphate springs occur across the island.

Cold springs (<30°C) were sampled from the Rembokola and Poghorovorughala catchments (near to the Eastern and Crater Wall thermal areas, respectively; Fig. 1), in both cases a short distance downstream of the major thermal areas. Cold springs (Table 4) are high pH (7.5–8.0), with low concentrations of most dissolved species. Calcium dominates the cation composition (40–150 mg/l), and sulphate is the major anion (100–300 mg/l). All species occur in lower concentrations in cold springs relative to hot springs from the same catchments, with the exception of Mg (8–13 mg/l). Cold spring samples cluster around $\delta^{18}O$ = −8‰ and δD = −45‰. The cold springs lie just above the global meteoric water line, and overlap with compositions of waters collected from wells and the Tanginakulu bicarbonate–sulphate spring (Fig. 4).

Data for the range of meteoric water isotope compositions in the Solomon Islands are unavailable, but comparison with data from Madang, Papua New Guinea (GNIP, 2006) suggests that the values of Savo cold springs and wells (Table 5) are representative of an

average meteoric water composition for the south west Pacific (Madang varies from $\delta^{18}O$ = −14 to −2‰ and δD = −92 to −3‰; average −7, −46‰). Thus, for the purposes of the following discussion, the average isotopic composition of well and cold spring waters is interpreted as being representative of meteoric-derived groundwater on Savo.

4.4 Strontium Isotopes

$^{87}Sr/^{86}Sr$ values (Fig. 5) for all hot and cold springs (average = 0.70420 ± 9) overlap with the values for local rocks (average = 0.70414 ± 11, based on 14 samples ranging from basalt to trachyte; Smith et al., 2009). A seawater sample collected by the same method from offshore Savo has a $^{87}Sr/^{86}Sr$ value of 0.709164 ± 12 (the accepted value for modern seawater is 0.709211 ± 37; Elderfield 1986). Coastal wells analysed in this study have $^{87}Sr/^{86}Sr$ values slightly higher (0.70442–0.70467) than those of the inland springs.

4.5 Native Sulphur

Native sulphur collected from areas of steaming ground and fumarolic / solfataric activity shows negative $\delta^{34}S$ values, ranging from −4.2 to −5.9‰, lower than sulphate recovered from acid springs, and considerably lower than that of alkaline springs (Table 5; Fig. 3).

5 Discussion

5.1 Water Chemistry

Surface discharge from the hydrothermal system at Savo is dominated by alkaline sulphate-type springs. The features of these springs (high sulphate, high silica, moderate Na-K-Ca-Mg, high pH, low chloride) are unusual in that sulphate-rich, chloride-poor springs are typically acidic, steam-heated springs. This is not the case at Savo.

Near-neutral or alkaline fluids from hydrothermal areas are typically close to equilibrium with a secondary (hydrothermally altered) mineral assemblage (Giggenbach, 1988). Although

Savo's alkaline sulphate springs have neutral to alkaline pH and high silica (indicating a significant amount of water–rock reaction has taken place), they are not in water–rock equilibrium (Fig. 6; Giggenbach, 1988). Instead, the alkaline sulphate springs form a chord within the immature waters field, trending from the √Mg apex towards 260–300°C equilibrium. The alkaline sulphate springs plot close to the isochemical host rock dissolution field, but their high pH, and low Fe and Al contents rule out isochemical dissolution as the process governing their Na-K-Mg composition. Such a process is largely limited to highly acidic fluids (Giggenbach, 1988).

On Fig. 6, the ratio Na/K is controlled by exchange of alkalis between aqueous fluids and coexisting feldspars, and is the basis of a widely used chemical thermometer (Fournier, 1979; Truesdell, 1984). The K/Mg ratio is controlled by equilibration with chlorite and other Mg-containing clays, and with biotite at high temperatures (Ellis and Mahon, 1977). The Na/K ratio of a hydrothermal fluid is slower to re-equilibrate down-temperature than K/Mg, and as a result is less subject to progressive resetting upon ascent and discharge. The simplest explanation for the array of points produced by alkaline sulphate springs on Fig. 6 (with relatively homogeneous Na/K, but variable Mg) is that the alkaline sulphate waters have equilibrated at 260–300°C and been subject to variable addition of more Mg-rich (cooler) waters.

Further evidence for fluid mixing and particular dilution of the alkaline sulphate waters comes from a comparison of various chemical thermometers. Na/K temperatures are much higher (260–300°C) than those derived from quartz solubility (Truesdell, 1984), and sulphate oxygen isotope (McKenzie and Truesdell, 1977) thermometers (Fig. 7). The two latter thermometers are affected by dilution, with a slight reduction in silica contents expected as cold waters are added, and a shift to lower δ^{18}_{H2O} affecting the sulphate oxygen calculation.

The thermometer discrepancies indicate that the alkaline sulphate fluids have been subject to significant mixing and dilution by a more Mg-rich, and therefore presumably cooler water, with lower $\delta^{18}O$, such as that discharged from cold springs (SV520, Table 4).

Further evidence of mixing is displayed on Fig. 8. The Eastern and Crater Wall alkaline sulphate springs define complex mixing lines, with the former towards a hydrothermal end-member, and the latter closer in composition to bicarbonate–sulphate and cold springs. Conservative elements such as Cl, Li, and Na (also B, K, Cs, Rb, and As; not shown on plots) show simple, straight-line dilution trends from Eastern to Crater Wall. These elements are present in higher concentrations in hydrothermal fluids because they are leached from the host rocks. Conversely, Mg is higher in low temperature fluids, as the formation of minerals such as chlorite rapidly removes it from high temperature fluids (Giggenbach, 1988). As a result, mixing leads to an increase from Eastern to Crater Wall. Bicarbonate also increases, most likely as a result of the higher solubility of CO_2 in cooler waters.

Sulphate has a complicated relationship with fluid mixing. Simple analysis of spring compositions with SOLVEQ (Reed, 1982; Reed and Spycher, 1984; ignoring boiling and volatile loss) indicates that the Eastern springs are saturated with anhydrite at approximately 120°C, whereas the Crater Wall springs are saturated at the discharge temperature of 100°C, and both are significantly lower than the 260–300°C Na/K temperature. This indicates that either sulphate, or more likely Ca (Fig. 8) has been added to the fluids post- Na/K equilibrium – anhydrite should become progressively undersaturated as the waters cool. The low saturation temperatures suggest the presence of anhydrite in the subsurface. Addition of cooler water encourages anhydrite dissolution and therefore maintains high sulphate concentrations in the springs. This process is discussed more fully in the following section.

Near surface boiling also affects the hot spring composition, most notably pH. Again using SOLVEQ (Reed, 1982; Reed and Spycher, 1984) to determine mineral saturations, calcite was supersaturated at discharge temperature (Log Q/K≈1.3 for Crater Wall, 0.2–0.6 for Eastern springs). Such supersaturation cannot be maintained at or above these temperatures (Palandri and Reed, 2001), suggesting that there has been CO_2 loss and an according rise in pH due to boiling. This process is at least partly responsible for the high pH of the spring waters. Springs are often surrounded by an apron of travertine and sinter as a result of the supersaturation of calcite (due to boiling and pH increase) and amorphous silica (due to cooling upon discharge).

Steaming ground and acid sulphate springs are further evidence of subsurface boiling at Savo. The acid springs at Savo are typical of steam-heated springs reported from other locations, in both physical appearance, setting, chemistry and stable isotope composition. Both acid and alkaline springs occur in close proximity, presumably physically separated by a boiling/ steam-heated zone, with the acid springs perched above this zone at the surface.

The final class of thermal spring that occurs at Savo is bicarbonate–sulphate type. Similar springs are relatively common in geothermal areas, occurring in parts of the system where CO_2 condenses into cold groundwater (Ellis and Mahon, 1977), either at depth or at the periphery of steam-heated areas. At Savo, sulphate is derived from small amounts of mixing with other sulphate-rich fluids, principally the alkaline sulphate type fluid (given the similar isotopic composition of the different spring types; Fig. 3). The elevated Ca and Mg concentrations indicate that the bicarbonate–sulphate water discharged at these springs has undergone moderate to low temperature (<100°C) reaction with the host rocks.

The sulphate content of these springs indicates that mixing with hydrothermal fluids occurs. This is unsurprising, given the Mg contents of the alkaline sulphate springs indicates the

same process. Evidence of mixing in both the high and low temperature fluids points towards the system at Savo being relatively "open"– that is, multiple fluid end-members are represented, but they mix freely, and as such, a spectrum of fluids are discharged.

5.1.1 Geochemical Modelling

As dilution, in terms of the elemental fluid chemistry, is a good candidate process for generating high sulphate, high silica, low chloride fluids at Savo, itwas investigated further by modelling the geochemical reactions of a simplified hydrothermal system with CHILLER (Reed, 1982; Reed, 1998). For this, two end member fluids were used (Table 6)– the chloride-rich fluid (based on a condensate from Augustine volcano mixed 1:10 with pure water; Reed, 1997; Symonds et al., 1990) and a synthetic chloride-poor, sulphate rich fluid (Reed, 1997). The simulation took these fluids and in separate runs, reacted them with an unaltered sodic trachyte (SV17; Smith et al., 2009) at 300°C to produce two rock-equilibrated fluids – one chloride rich, the other chloride poor. These were then used in a simulation of dilution. In this case, 300°C pure water was added to the fluid and its associated secondary mineral assemblage (Table 6).

Comparison of the high and low chloride models indicates a number of common characteristics (Table 6, Fig. 9). As dilution increases: there is a small pH increase (Table 6); a significant decrease in the concentrations of Cl^- and HCO_3^-; and dissolved SiO_2 remains relatively unchanged. Dissolved SO_4^{2-} and HS^- increase until the controlling mineral phases (anhydrite and pyrite respectively) have been consumed. Aqueous silica remains relatively constant due to the abundance of quartz in the secondary mineral assemblage. The extended run for the high chloride system (Fig. 9) in particular displays this phenomenon, with a marked inflection in the trend of SO_4^{2-} concentration when anhydrite is exhausted; once the controlling mineral is gone, the dissolved components are diluted at a 1:1 ratio (as for Cl^-).

Though isothermal dilution is a simplification of the actual process, these simulations demonstrate that simple dilution, when "buffered" by a mineral assemblage, is a plausible explanation for reducing the chloride content of a hydrothermal fluid whilst maintaining or even enhancing concentrations of sulphate and silica.

The chemistry of the alkaline sulphate springs suggests considerable fluid mixing and dilution, probably with a cooler water on the basis of the high Mg^{2+} concentrations. The abundance of cooler waters to dilute the hydrothermal system is most likely a result of the tropical climate of the Solomon Islands and high annual rainfall (3–5 m; Solomon Islands Meteorological Service).

5.2 Oxygen and Hydrogen Isotopes of Water

The alkaline sulphate springs discharge rapidly, and the residence time of any mass of water in the spring is short. Thus, the isotopic composition of the fluids is unlikely to be affected by post-discharge evaporation. Two exceptions to this are the outliers shown on Fig. 4 (SV207 and 208), that appear to have undergone evaporative enrichment similar to the acid springs (see below).

The position of the alkaline sulphate springs on Fig. 4 can be produced by a number of different (although not mutually exclusive) processes. On $\delta^{18}O$–δD plots, the condensation of magmatic vapour into meteoric-derived groundwater produces a straight mixing line between the two end-member compositions (Hedenquist and Aoki, 1991). However, the chemistry of the springs (high pH, low chloride) is inconsistent with such an origin, thus meteoric–magmatic mixing is unlikely to be the sole process determining the isotopic composition of the alkaline sulphate springs. Water–rock reaction produces horizontal shifts in $\delta^{18}O$–δD space, whilst boiling causes minor increase of δD (Fig. 4; Giggenbach and Stewart, 1982). The latter two processes can be demonstrated to occur at Savo (sections 5.1 and 5.1.1), whilst

the addition of magmatic volatiles is likely based on the high temperatures (300°C Na/K temperature) and sulphur contents of the fluids. That the $\delta^{18}O$ and δD values of the springs are relatively close to the meteoric composition, despite high temperature water–rock reaction and presumed addition of magmatic volatiles is further evidence that the system at Savo is subject to dilution and flushing with fresh water.

The acid sulphate springs analysed at Savo (plus two of the outliers from the alkaline sulphate cluster) lie on a trend with a slope close to 3 with an origin at local meteoric, suggesting evaporation is the dominant control on the oxygen and hydrogen isotopic composition on these springs (Fig. 4; Craig 1963).

5.3 Sulphur Isotopes and Sources of Sulphate

In magmatic-hydrothermal systems sulphate-rich fluids are generally produced by two processes: condensation of primary magmatic volatiles, including SO_2, into groundwater; or oxidation of H_2S from a secondary steam phase in surface waters:

$$4SO_2 + 4H_2O = 3H_2SO_4 + H_2S \quad (1)$$

$$H_2S + 2O_2 = H_2SO_4 \quad (2)$$

The first reaction involves the disproportionation of magmatic SO_2 upon reaction with water at temperatures below about 350°C (Holland, 1965). Isotopic fractionation results in H_2SO_4 being enriched in ^{34}S, and the H_2S depleted in ^{34}S (Ohmoto and Rye, 1979). This H_2S may eventually be oxidised at the surface as in equation 2 to produce native sulphur or sulphate depleted in ^{34}S relative to the bulk sulphur value for the magma (Rye, 1993).

The isotopic composition of native sulphur from fumaroles, as well as sulphate from acid springs, should be representative of the H_2S within the system. The oxidation of H_2S at the surface (equation 2) approximately preserves the sulphur isotope signature of the H_2S (Rye et al., 1992). Mixing with high-$\delta^{34}S$ fluids (such as alkaline sulphate-fed streams) increases the

values in the acid sulphate springs and accounts for the spread of data away from the negative native sulphur values.

Comparison of the H_2S proxies and alkaline sulphate $\delta^{34}S$ shows that they are far from isotopic equilibrium (calculated equilibrium temperature is >600°C; Ohmoto and Rye, 1979). Two processes can account for this. One is that sulphur isotope equilibrium is only slowly attained at high pH (Ohmoto and Lasaga, 1982), and so if high pH fluids dominate the subsurface of Savo (as they do the surface) then sulphur isotope equilibrium is unlikely to occur. A second explanation is that pyrite and other sulphides are re-dissolved by relatively oxidising waters "flushing" the system, which moves the sulphate composition towards lower values.

Seawater contamination can be ruled out as a source of ^{34}S-enriched sulphate to the alkaline springs – chloride and $^{87}Sr/^{86}Sr$ values are inconsistent with any significant (>1%) marine contributions (Fig. 5).

Importantly, the sulphur isotope date show that the alkaline springs are unlikely to represent evolved steam-heated waters that have attained isotopic equilibration between sulphate and sulphide/H_2S, given the time required for equilibration is approximately 10,000 years, at pH 7 and temperatures <150°C (Rye et al., 1992).

5.4 Comparison with Other Springs

Although sulphate-rich, chloride-poor fluids are found at many springs worldwide, typically they are steam-heated acid sulphate springs. Higher pH sulphate-rich springs are rarely recorded in the literature. Table 7 contains water chemistry data for a number of moderate to high pH sulphate springs. However, unlike Savo, the waters recorded in Table 7 are not the dominant water type discharging from their respective hydrothermal systems – acid sulphate and/or chloride-rich waters dominate in all four examples.

The Black Pool in the crater of El Chichón, Mexico, is a muddy, closed pool, with a temperature and chemical composition similar to the alkaline sulphate springs of Savo, but with a slightly acidic pH. Taran et al. (1998) observe that the spring is dilute, but compare its chemistry to steam-heated acid-sulphate springs within the volcanic crater, implying a steam-heated origin. Sulphur isotopes can be used to distinguish the steam-heated and alkaline sulphate springs at Savo, and dilution of an acid sulphate spring cannot account for the high SiO_2 and consistent (high) Na/K temperatures of the alkaline springs.

Stimac et al. (2004) suggest a steam and gas condensation origin for the (pre-1991 eruption) Upper Maranout springs of Pinatubo, as do Giggenbach et al. (1990) for Las Nereidas springs of Nevado del Ruiz (Colombia). These springs, with elevated bicarbonate concentrations, are more similar in chemistry to the cooler bicarbonate-sulphate springs of Savo. At Pinatubo, Ruiz and Savo, the bicarbonate-enriched springs are peripheral to the high temperature fluids, and have relatively low temperatures. At Savo, sulphate would appear to be derived from mixing with alkaline sulphate fluids rather than from oxidation of H_2S, based on their stable isotope compositions ("Other springs"; Fig. 3) as compared to the native sulphur, acid and alkaline springs.

Thjórsárdalur spring (Table 7), is from an area of high gas flux on Iceland. Arnórsson et al. (1983) suggested its high-sulphate chemistry is formed by the dissolution and oxidation of secondary pyrite. This process is not dissimilar to the process as envisaged at Savo, with the dissolution of secondary hydrothermal alteration assemblages buffering the fluid composition during dilution. Sulphur isotopes from the alkaline sulphate springs suggest that anhydrite and sulphate derived from SO_2 disproportionation contributes to the springs at Savo, rather than exclusively the oxidation of pyrite – which would result in similar isotopic compositions between native sulphur, acid sulphate and alkaline springs.

In summary, dilution plays an important role in the springs listed in Table 7, driving the pH to higher values whilst maintaining low chloride concentrations. However, most of the fluids in Table 7 formed in relatively shallow, peripheral areas, mostly by steam-heated processes. The alkaline sulphate springs at Savo are from a hotter, deeper system (i.e. they are hypogene fluids), as indicated by the sulphur isotopes, Na/K characteristics, high temperatures, and high SiO_2 concentrations.

6 Conclusions

The hydrothermal system of Savo volcano is manifested at the surface by a number of hot spring types. The dominant spring type is of an unusual alkaline sulphate-type composition, characterised by dilute, high pH (7–8), low chloride (<50 mg/l), high sulphate (>600 mg/l) and high silica (>250 mg/l) waters. They have $\delta^{34}S_{SO4}$ values clustered around 5.4 (± 1.5‰) and $\delta^{18}O_{H2O}$ values slightly more enriched than non-thermal groundwater (−4‰ and −8‰, respectively). The springs have relatively consistent Na/K thermometer temperatures of 260–300°C, indicating a hot, deep, hypogene origin. A smaller number of acid sulphate springs also occur, with distinct $\delta^{34}S_{SO4}$ values (−0.6 ± 2.5‰) compared to the alkaline sulphate fluids, higher $\delta^{18}O_{H2O}$ and δD_{H2O} values, and variable, but generally low pH (2–7), typical of steam-heated springs.

The unusual alkaline sulphate springs discharging at Savo volcano record a range of hydrothermal processes, including water–rock reaction, fluid mixing and the addition of magmatic volatiles. Initially sulphate-rich fluids, with an unknown chloride concentration, react and equilibrate with the host rock. Secondary minerals in this assemblage provide important buffers for the fluid composition (sulphate and silica in particular) as large amounts of cooler, fresh water are added to the system, most likely as a result of the tropical, high rainfall climate of Savo and the Solomon Islands.

Dilution is the key process whereby the alkaline sulphate fluids derive their high pH and high-sulphate, low-chloride chemistry. Mixing with dilute, meteoric-dominated, Ca–Mg-rich fluids results in spring discharges that only partially record reservoir conditions; at discharge the chemistry has been greatly modified from that which was presumably in equilibrium with a hydrothermal mineral assemblage at depth.

Low chloride in particular provides evidence for heavily diluted hydrothermal fluids. Sulphate is the major anion but responds differently to fluid mixing and dilution compared to chloride because it is to a certain extent controlled by precipitation and re-dissolution of sulphate and sulphide minerals in the subsurface.

Near-surface boiling contributes a final, small pH increase as volatile species (CO_2 and possibly H_2S) are degassed. Fluids are saturated with various minerals at the surface, notably calcite and amorphous silica, leading to the precipitation of travertine and sinter deposits.

A wide range of groundwater compositions is exhibited at Savo (alkaline sulphate, acid sulphate, bicarbonate–sulphate and cold springs), but evidence for mixing between these types, both at the surface and in the subsurface, is strong. As such, Savo represents a relatively open system.

Common hydrothermal processes have combined at Savo to produce unusual fluid chemistry. High rainfall increases the effectiveness and likelihood of fluid mixing. Savo displays geological features similar to meteoric-dominated geothermal systems, including extensive sinter deposits and widespread steam-heated zones, but fluids discharge from the majority of the springs have an unusual chemistry. The recognition of features such as sinters and carbonate veins in an ancient hydrothermal setting is not necessarily diagnostic of neutral chloride fluids in a geothermal system environment – they may be produced in a Savo-like, low chloride, diluted magmatic-hydrothermal system.

7 Acknowledgements

This research was funded by the Natural Environment Research Council (UK) and British Geological Survey University Funding Initiative as part of PhD studentship NER/S/A/2004/12339. Analytical work was supported by NERC Isotope Geosciences Facilities Steering Committee grant IP/889/1105. The Society of Economic Geologists Student Research Grants (Hugh E. McKinstry and Newmont Mining Corporation funds) provided support for fieldwork. This manuscript benefitted from reviews and comments by Mark H. Reed (U. Oregon), Jeremy Fein (U. Notre Dame) and an anonymous reviewer. The authors would like to thank A. McDonald, J. Dougans, C. Taylor and A. Tait (SUERC); K. Green and RA. Shaw (BGS); A. Sumner (NIGL); W. Satokana, G. Albert, A. Ramo, D. Billy and S. Basi (Solomon Islands Ministry of Natural Resources); the British High Commission (Honiara); SJ Cronin and K Németh (Massey University); and A Rankin (Kingston University, London). JN, MGP, WGD, HT and ILM publish with the permission of the Executive Director, British Geological Survey (NERC).

8 References

Arnórsson, S. (Editor), 2000. Isotopic and Chemical Techniques in Geothermal Exploration, Development and Use: Sampling Methods, Data Handling, Interpretation International Atomic Energy Agency, Vienna.

Arnórsson, S., Gunnlaugsson, E. and Svavarsson, H., 1983. The chemistry of geothermal waters in Iceland. II. Mineral equilibria and independent variables controlling water compositions. Geochimica et Cosmochimica Acta, 47(3): 547-566.

Ault, L., Green, K.A. and Perkins, K.M., 1999. Validation of the procedure for the determination of major and trace cations in aqueous samples by inductively coupled plasma-atomic emission spectrometry (Fisons/ARL 3580). British Geological Survey Technical Report WI/00/6.

Charlton, B.D., Reeder, S. and Watts, M.J., 2003. Method validation for the determination of major and trace anions by Ion Chromatography (DX-600). British Geological Survey Internal Report IR/03/79.

Coleman, M.L. and Moore, M.P., 1978. Direct reduction of sulfates to sulfur dioxide for isotopic analysis. Analytical Chemistry, 50(11): 1594-1595.
Cook, J.M., Robinson, J.J., Chenery, S.R.N. and Perkins, K.M., 2002. Validation report for the analysis of aqueous solutions by ICP-MS, AGN 2.3.3. British Geological Survey Internal Report IR/02/091R.
Coplen, T.B., Hopple, J.A., Böhlke, J.K., Peiser, H.S., Rieder, S.E., Krouse, H.R., Rosman, K.J.R., Ding, T., Vocke Jr, R.D., Révész, K.M., Lamberty, A., Taylor, P. and De Bièvre, P., 2002. Compilation of minimum and maximum isotope ratios of selected elements in naturally occurring terrestrial materials and reagents. USGS Water Resources Investigation Report 01-4222.
Delmelle, P., Bernard, A., Kusakabe, M., Fischer, T.P. and Takano, B., 2000. Geochemistry of the magmatic-hydrothermal system of Kawah Ijen Volcano, East Java, Indonesia. Journal of Volcanology and Geothermal Research, 97: 31-53.
Donnelly, T., Waldron, S., Tait, A., Dougans, J. and Bearhop, S., 2001. Hydrogen isotope analysis of natural abundance and deuterium-enriched waters by reduction over chromium on-line to a dynamic dual inlet isotope-ratio mass spectrometer. Rapid Communications in Mass Spectrometry, 15(15): 1297-1303.
Elderfield, H., 1986. Strontium isotope stratigraphy. Palaeogeography, Palaeoclimatology, Palaeoecology, 57(1): 71-90.
Ellis, A.J. and Mahon, W.A.J., 1977. Chemistry and Geothermal Systems. Academic Press, New York, 392 pp.
Epstein, S. and Mayeda, T., 1953. Variation of O^{18} content of waters from natural sources. Geochimica et Cosmochimica Acta, 4(5): 213-224.
Fournier, R.O., 1979. A revised equation for the Na/K geothermometer. Geothermal Resources Council Transactions, 3: 221-224.
Giggenbach, W.F., 1988. Geothermal solute equilibria: Derivation of Na-K-Mg-Ca geoindicators. Geochimica et Cosmochimica Acta, 52(12): 2749-2765.
Giggenbach, W.F., 1992. Isotopic shifts in waters from geothermal and volcanic systems along convergent plate boundaries and their origin. Earth and Planetary Science Letters, 113(4): 495-510.
Giggenbach, W.F., 1997. The origin and evolution of fluids in magmatic-hydrothermal systems. In: H.L. Barnes (Editor), Geochemistry of Hydrothermal Ore Deposits, 3rd Edition. John Wiley and Sons, pp. 737-796.
Giggenbach, W.F., Garcia P., N., Londono C., A., Rodriguez V., L., Rojas G., N. and Calvache V., M.L., 1990. The chemistry of fumarolic vapor and thermal-spring discharges from the Nevado del Ruiz volcanic-magmatic-hydrothermal system, Colombia. Journal of Volcanology and Geothermal Research, 42(1-2): 13-39.
Giggenbach, W.F., Shinohara, H., Kusakabe, M. and Ohba, T., 2003. Formation of acid volcanic brines through interaction of magmatic gases, seawater, and rock within the White Island volcanic-hydrothermal system, New Zealand. In: S.F. Simmons and I. Graham (Editors), Volcanic, Geothermal and Ore-Forming Fluids: Rulers and Witnesses of Processes within the Earth. Special Publication No. 10. Society of Economic Geologists, Littleton, Colorado, pp. 19-40.
Giggenbach, W.F. and Stewart, M.K., 1982. Processes controlling the isotopic composition of steam and water discharges from steam vents and steam-heated pools in geothermal areas. Geothermics, 11(2): 71-80.
Grover, J.C., 1958. Savo volcano - a potential danger to its inhabitants, The Solomon Islands - geological exploration and research, 1953 - 56. Geological Survey of the British Solomon Islands Memoir, pp. 108-111.

Hall, A.J., Boyce, A.J., Fallick, A.E. and Hamilton, P.J., 1991. Isotopic evidence of the depositional environment of Late Proterozoic stratiform barite mineralization, Aberfeldy, Scotland. Chemical Geology, 87(2): 99-114.

Hedenquist, J.W. and Aoki, M., 1991. Meteoric interaction with magmatic discharges in Japan and the significance for mineralization. Geology, 19(10): 1041-1044.

Henley, R.W. and Ellis, A.J., 1983. Geothermal systems ancient and modern: a geochemical review. Earth-Science Reviews, 19(1): 1-50.

Holland, H.D., 1965. Some applications of thermochemical data to problems of ore deposits; Part 2, Mineral assemblages and the composition of ore forming fluids. Economic Geology, 60(6): 1101-1166.

IAEA/WMO, 2006. Global Network of Isotopes in Precipitation Database. The GNIP Database. Accessible at http://isohis.iaea.org.

Johnson, R.W., Jaques, A.L., Langmuir, C.H., Perfit, M.R., Staudigel, H., Dunkley, P.N., Chappell, B.W., Taylor, S.R. and Baekisapa, M., 1987. Ridge subduction and forearc volcanism; petrology and geochemistry of rocks dredged from the western Solomon Arc and Woodlark Basin. In: B. Taylor and N.F. Exon (Editors), Marine Geology, Geophysics and Geochemistry of the Woodlark Basin-Solomon Islands. Circum-Pacific Council for Energy and Mineral Resources, Earth Science Series, pp. 155-226.

König, S., Schuth, S., Münker, C. and Qopoto, C., 2007. The role of slab melting in the petrogenesis of high-Mg andesites: evidence from Simbo Volcano, Solomon Islands. Contributions to Mineralogy and Petrology, 153(1): 85-103.

Kornexl, B.E., Werner, R.A. and Gehre, M., 1999. Standardization for oxygen isotope ratio measurement - still an unsolved problem. Rapid Communications in Mass Spectrometry, 13(13): 1248-1251.

Lipfert, G., Sidle, W.C., Reeve, A.S., Ayuso, R.A. and Boyce, A.J., 2007. High arsenic concentrations and enriched sulfur and oxygen isotopes in a fractured-bedrock ground-water system. Chemical Geology, 242: 385-399.

McInnes, B.I.A., Gregoire, M., Binns, R.A., Herzig, P.M. and Hannington, M.D., 2001. Hydrous metasomatism of oceanic sub-arc mantle, Lihir, Papua New Guinea: petrology and geochemistry of fluid-metasomatised mantle wedge xenoliths. Earth and Planetary Science Letters, 188(1-2): 169-183.

McKenzie, W.F. and Truesdell, A.H., 1977. Geothermal reservoir temperatures estimated from the oxygen isotope compositions of dissolved sulfate and water from hot springs and shallow drillholes. Geothermics, 5(1-4): 51-61.

Müller, D., Franz, L., Herzig, P.M. and Hunt, S., 2001. Potassic igneous rocks from the vicinity of epithermal gold mineralization, Lihir Island, Papua New Guinea. Lithos, 57(2-3): 163-186.

Ohmoto, H. and Lasaga, A.C., 1982. Kinetics of reactions between aqueous sulfates and sulfides in hydrothermal systems. Geochimica et Cosmochimica Acta, 46(10): 1727-1745.

Ohmoto, H. and Rye, R.O., 1979. Isotopes of sulfur and carbon. In: H.L. Barnes (Editor), Geochemistry of Hydrothermal Ore Deposits, 2nd Edition. John Wiley and Sons, pp. 509-567.

Palandri, J.L. and Reed, M.H., 2001. Reconstruction of in situ composition of sedimentary formation waters. Geochimica et Cosmochimica Acta, 65(11): 1741-1767.

Petterson, M.G., Babbs, T., Neal, C.R., Mahoney, J.J., Saunders, A.D., Duncan, R.A., Tolia, D., Magu, R., Qopoto, C., Mahoa, H. and Natogga, D., 1999. Geological-tectonic framework of Solomon Islands, SW Pacific; crustal accretion and growth within an intra-oceanic setting. Tectonophysics, 301(1-2): 35-60.

Petterson, M.G., Cronin, S.J., Taylor, P.W., Tolia, D., Papabatu, A., Toba, T. and Qopoto, C., 2003. The eruptive history and volcanic hazards of Savo, Solomon Islands. Bulletin of Volcanology, 65(2-3): 165-181.

Phinney, E.J., Mann, P., Coffin, M.F. and Shipley, T.H., 2004. Sequence stratigraphy, structural style, and age of deformation of the Malaita accretionary prism (Solomon arc–Ontong Java Plateau convergent zone). Tectonophysics, 389(3-4): 221-246.

Reed, M.H., 1982. Calculation of multicomponent chemical equilibria and reaction processes in systems involving minerals, gases and an aqueous phase. Geochimica et Cosmochimica Acta, 46(4): 513-528.

Reed, M.H., 1997. Hydrothermal alteration and its relationship to ore fluid composition. In: H.L. Barnes (Editor), Geochemistry of Hydrothermal Ore Deposits, 3rd Edition. John Wiley and Sons, pp. 303-366.

Reed, M.H., 1998. Calculation of simultaneous chemical equilibria in aqueous-mineral-gas systems and its application to modeling hydrothermal processes. In: J. Richards and P. Larson (Editors), Techniques in Hydrothermal Ore Deposits Geology. Reviews in Economic Geology. Society of Economic Geologists, pp. 109-124.

Reed, M.H. and Spycher, N., 1984. Calculation of pH and mineral equilibria in hydrothermal waters with application to geothermometry and studies of boiling and dilution Geochimica et Cosmochimica Acta, 48(7): 1479-1492.

Richards, J.P., Chappell, B.W. and McCulloch, M.T., 1990. Intraplate-type magmatism in a continent island-arc collision zone: Porgera intrusive complex, Papua New Guinea. Geology, 18: 958-961.

Robinson, B.W. and Kusakabe, M., 1975. Quantitative Preparation of Sulfur-Dioxide, for ^{34}S-^{32}S Analyses, from Sulfides by Combustion with Cuprous-Oxide. Analytical Chemistry, 47(7): 1179-1181.

Royse, K.R., Kempton, P.D. and Darbyshire, D.P.F., 1998. Procedure for the analysis of rubidium-strontium and samarium-neodymium isotopes at the NERC Isotope Geosciences Laboratory. NIGL Report Series No. 121.

Rye, R.O., 1993. The evolution of magmatic fluids in the epithermal environment; the stable isotope perspective. Economic Geology, 88(3): 733-752.

Rye, R.O., Bethke, P.M. and Wasserman, M.D., 1992. The stable isotope geochemistry of acid sulfate alteration. Economic Geology, 87(2): 225-262.

Smith, D.J., 2008. From Slab to Sinter: The Magmatic-Hydrothermal System of Savo Volcano, Solomon Islands. Ph.D. Thesis, University of Leicester.

Smith, D.J., Petterson, M.G., Saunders, A.D., Millar, I.L., Jenkin, G.R.T., Toba, T., Naden, J. and Cook, J.M., 2009. The petrogenesis of sodic island arc magmas at Savo volcano, Solomon Islands. Contributions to Mineralogy and Petrology, 158(6): 785-801.

Stimac, J.A., Goff, F., Counce, D., Larocque, A.C.L., Hilton, D.R. and Morgenstern, U., 2004. The crater lake and hydrothermal system of Mount Pinatubo, Philippines: evolution in the decade after eruption. Bulletin of Volcanology, 66(2): 149-167.

Symonds, R.B., Rose, W.I., Gerlach, T.M., Briggs, P.H. and Harmon, R.S., 1990. Evaluation of gases, condensates, and SO_2 emissions from Augustine volcano, Alaska: the degassing of a Cl-rich volcanic system. Bulletin of Volcanology, 52: 355-374.

Taran, Y., Fischer, T.P., Pokrovsky, B., Sano, Y., Armienta, M.A. and Macias, J.L., 1998. Geochemistry of the volcano-hydrothermal system of El Chichón Volcano, Chiapas, Mexico. Bulletin of Volcanology, 59(6): 436-449.

Truesdell, A.H., 1984. Chemical geothermometers for geothermal exploration. In: R.W. Henley, A.H. Truesdell and P.B. Barton Jr. (Editors), Fluid-Mineral Equilibria in Hydrothermal Systems. Society of Economic Geologists, pp. 31-44.

Truesdell, A.H., Nathenson, M. and Rye, R.O., 1977. The effects of subsurface boiling and dilution on the isotopic compositions of Yellowstone thermal waters. Journal of Geophysical Research, B, Solid Earth and Planets, 82(26): 3694-3704.

9 Tables

Table 1: Data for Crater Wall (Poghorovorughala valley) alkaline sulphate springs.

Table 2: Data for Eastern (Rembokola valley) alkaline sulphate springs.

Table 3: Data for acid sulphate springs.

Table 4: Data for bicarbonate–sulphate and cold springs.

Table 5: Isotope data for well water, native sulphur and igneous anhydrite samples.

Table 6: Fluid compositions from geochemical simulation of water–rock reaction and dilution processes.

Table 7: Fluid compositions from selected high sulphate, low chloride, near-neutral pH springs.

10 Figures

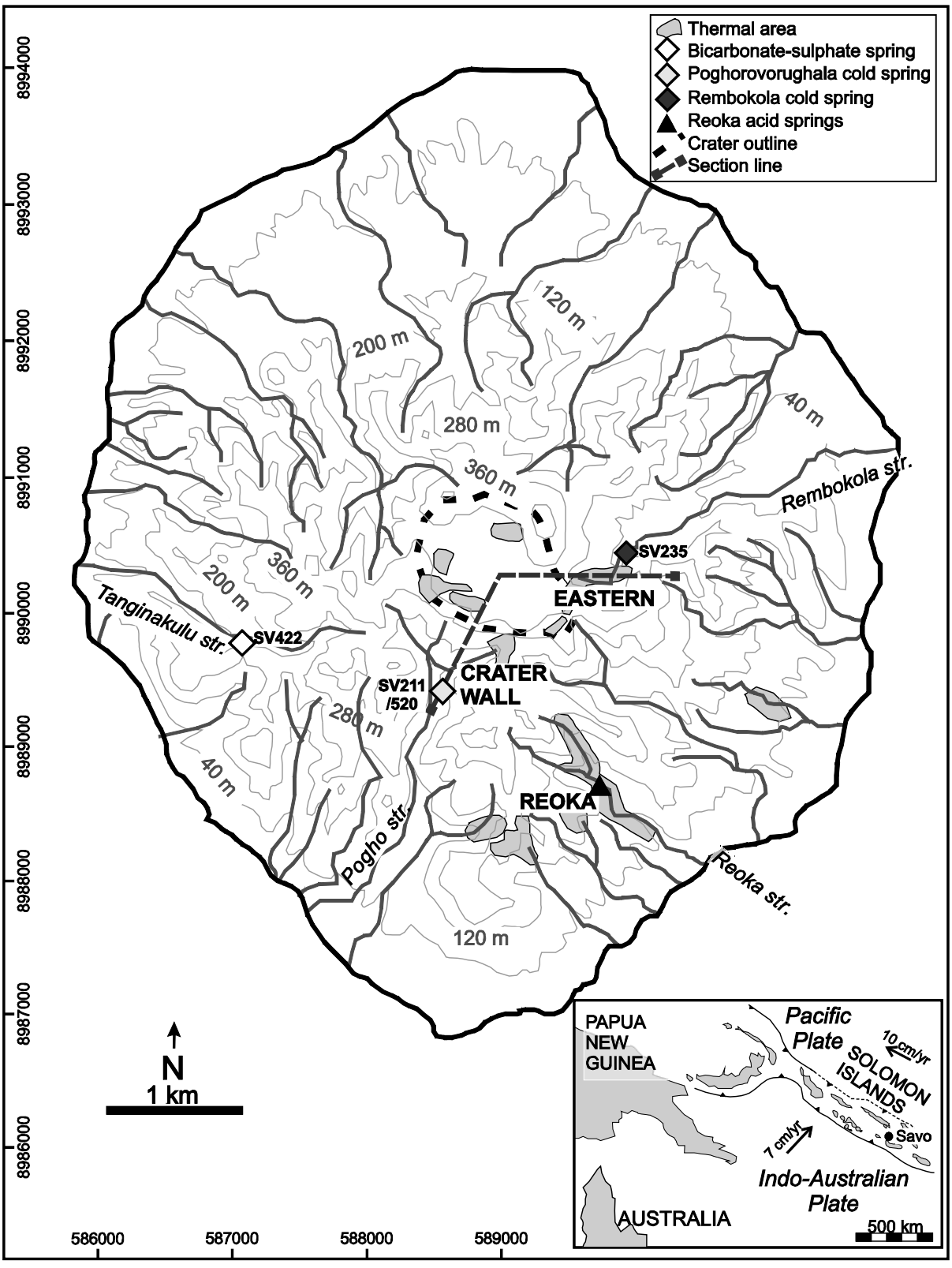

Fig. 1: Map of Savo Island showing location of major thermal areas, streams and some outlying spring samples. Thermal areas (springs, steaming ground, fumaroles and ground

temperature >30°C) are shaded; the major hot spring areas (Eastern and Crater Wall springs) are marked by text. Grid references are for UTM zone 57L. Inset shows major tectonic features in the southwest Pacific.

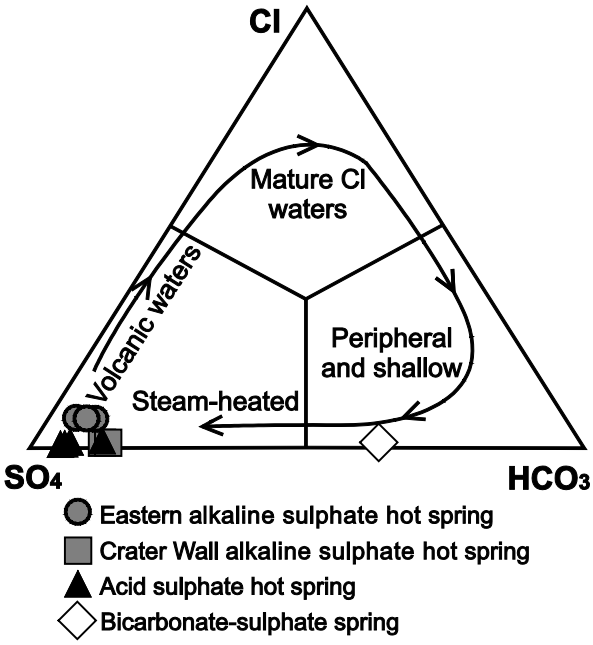

Fig. 2: Anion ternary with arrow showing Savo springs compared to general evolution of fluids in a magmatic hydrothermal system from initial magmatic sulphate dominated fluids to rock-buffered, neutral chloride “mature” fluids. Bicarbonate and steam-heated acid sulphate waters occur in the near surface and peripheral parts of hydrothermal system. Diagram after Giggenbach (1997).

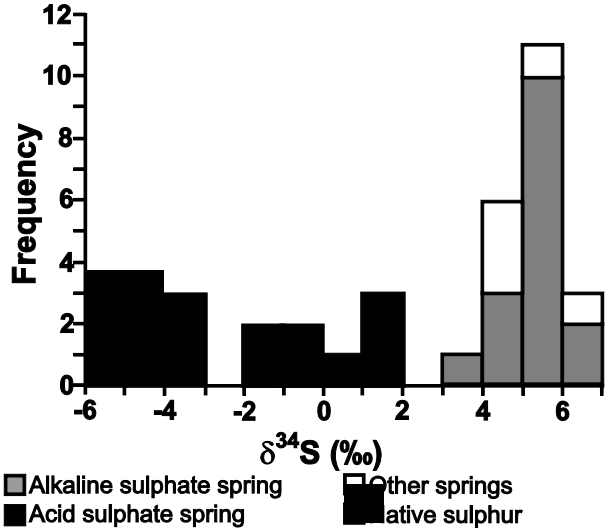

Fig. 3: Histogram of $\delta^{34}S$ values of spring sulphate and native sulphur samples from Savo.

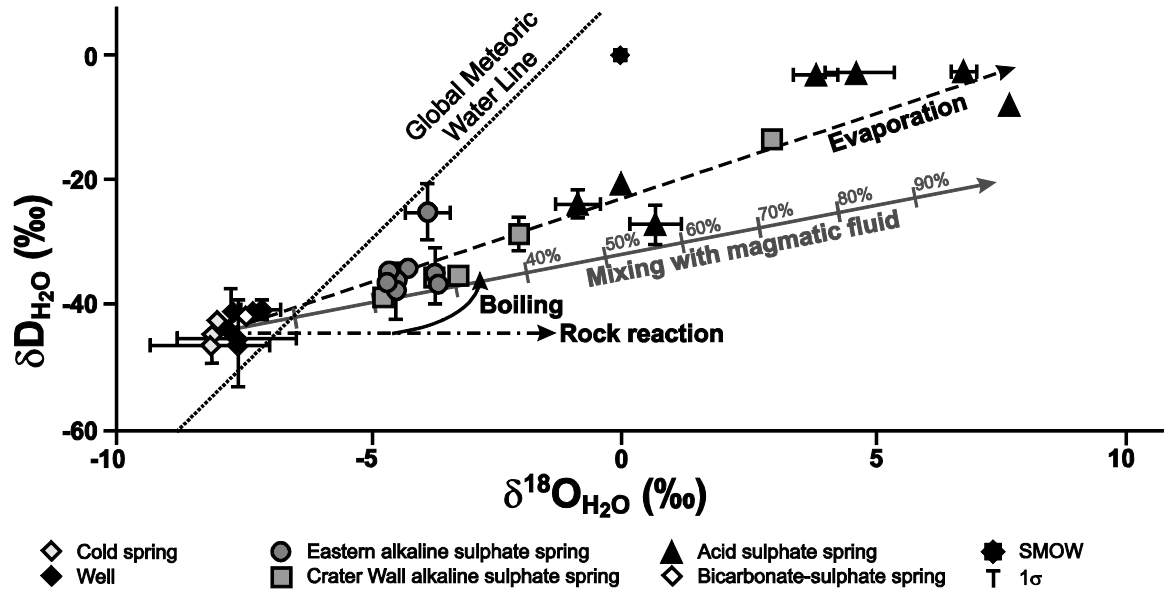

Fig. 4: δD_{H2O} vs. $\delta^{18}O_{H2O}$ for springs and wells. Error bars represent one standard deviation from mean value for samples analysed in triplicate; most are within symbol size. Arrows indicate enrichment trends produced by evaporation, particularly important for acid sulphate springs and alkaline sulphate outliers (the two samples to the right of the main cluster of alkaline sulphate data); mixing with a magmatic fluid; equilibration with host rocks; and boiling. Magmatic mixing trend uses fluid composition of δ18O = 6‰ (typical value for host rocks; Smith, 2009), δD = −20‰ ("andesitic water"; Giggenbach, 1992).

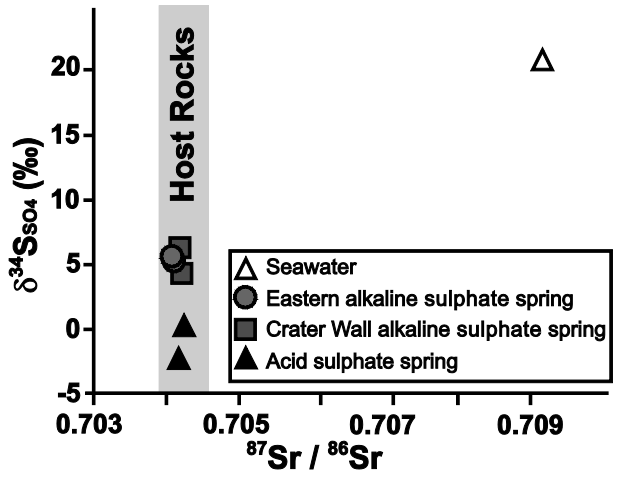

Fig. 5: $^{87}Sr/^{86}Sr$ versus $\delta^{34}S_{SO4}$ for hot springs and seawater (this study). Range of whole rock $^{87}Sr/^{86}Sr$ for local unaltered rocks also shown (Smith et al., 2009).

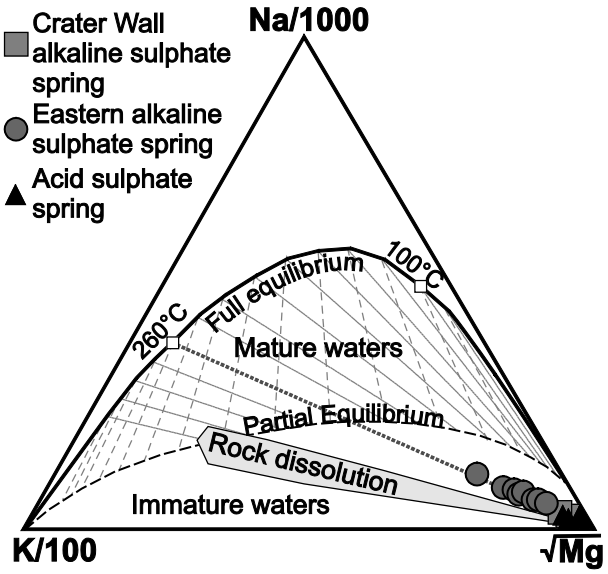

Fig. 6: Na–Mg–K ternary diagram, after Giggenbach (1988). Full equilibrium line plotted by intersection of Na/K and K/Mg isotherms (plotted at 20°C intervals as fine dotted and dashed lines respectively, 100° and 260°C intersections marked). Rock dissolution field shows fluid compositions expected by isochemical dissolution of unaltered host rock (trachytes and mugearites; Petterson et al., 2003; Smith et al., 2009). Hot spring waters from Savo plot as immature waters, but define a chord trending back towards 260–300°C equilibrium.

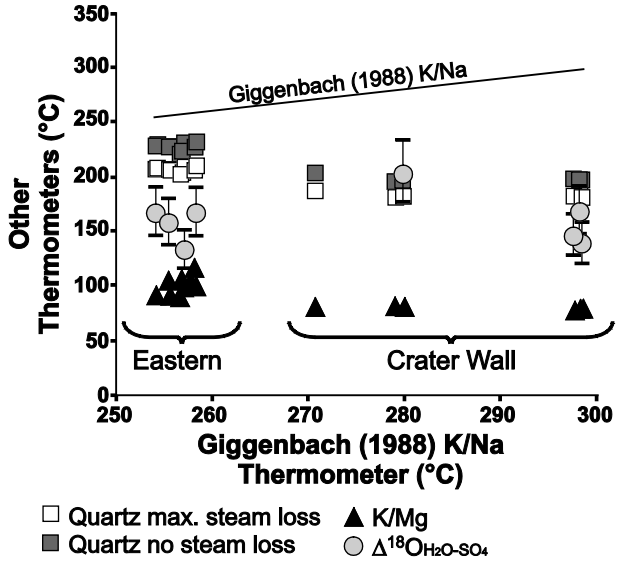

Fig. 7: Comparison of various chemical thermometry calculations on alkaline sulphate fluids. Horizontal axis uses values derived from the Giggenbach (1988) K/Na thermometer. Quartz thermometers are from Truesdell (1984), K/Mg from Giggenbach (1988), and $\Delta^{18}O_{SO4-H2O}$ thermometer from Truesdell et al. (1977). Error bars for K/Mg and quartz variants are within point size.

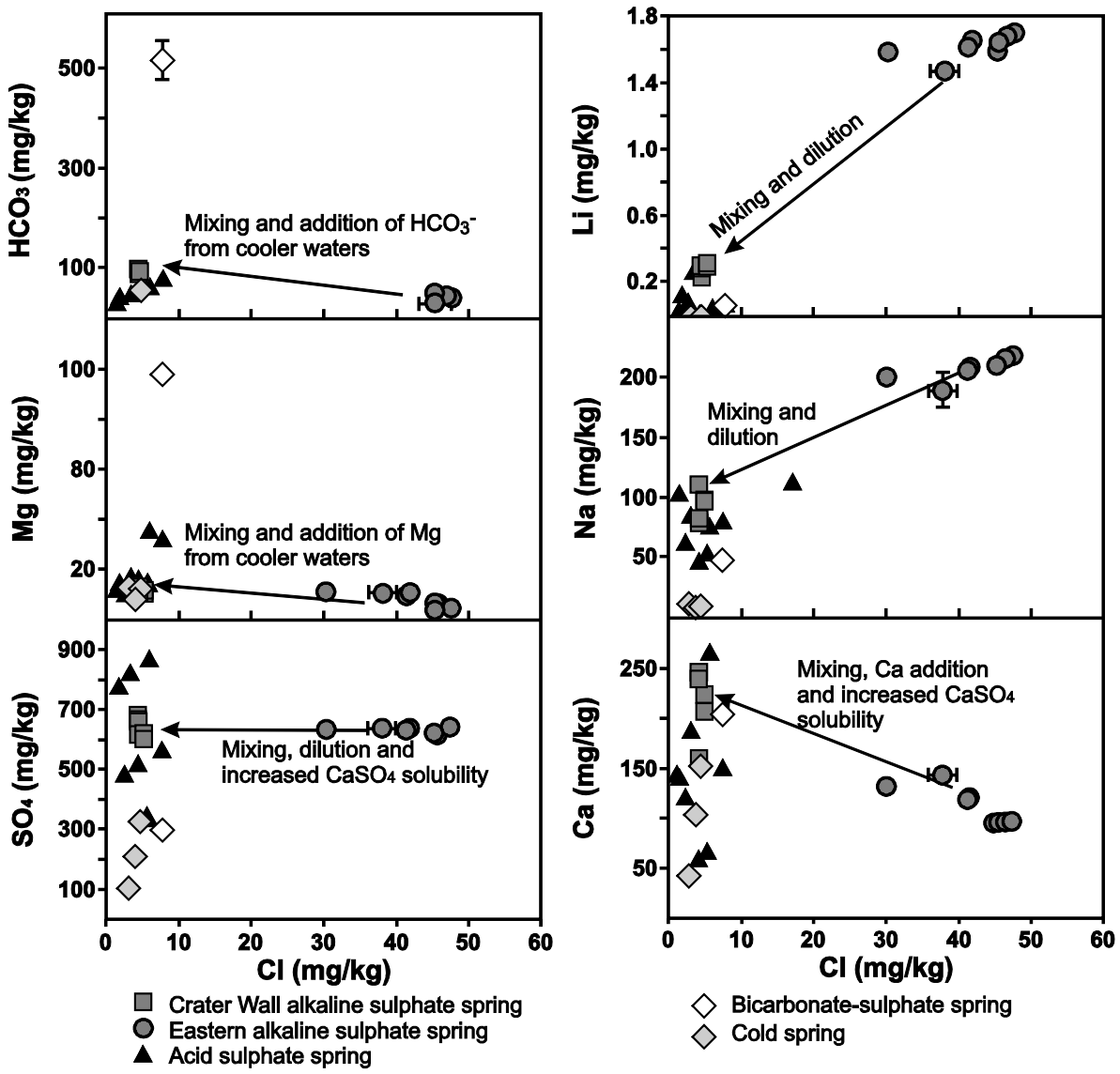

Fig. 8: Plots showing effects of mixing between fluid types at Savo. Typical error bars are shown for an Eastern spring and the bicarbonate–sulphate spring, although in most cases errors are within point size. Arrows show mixing trends indicated by relative differences between Eastern and Crater Wall alkaline sulphate hot springs. More conservative elements (Cl^-, Li, Na) show simple dilution trends, whereas Mg and HCO_3^- increase as the hydrothermal fluid mixes with cooler groundwater. Sulphate and Ca are buffered by anhydrite solubility.

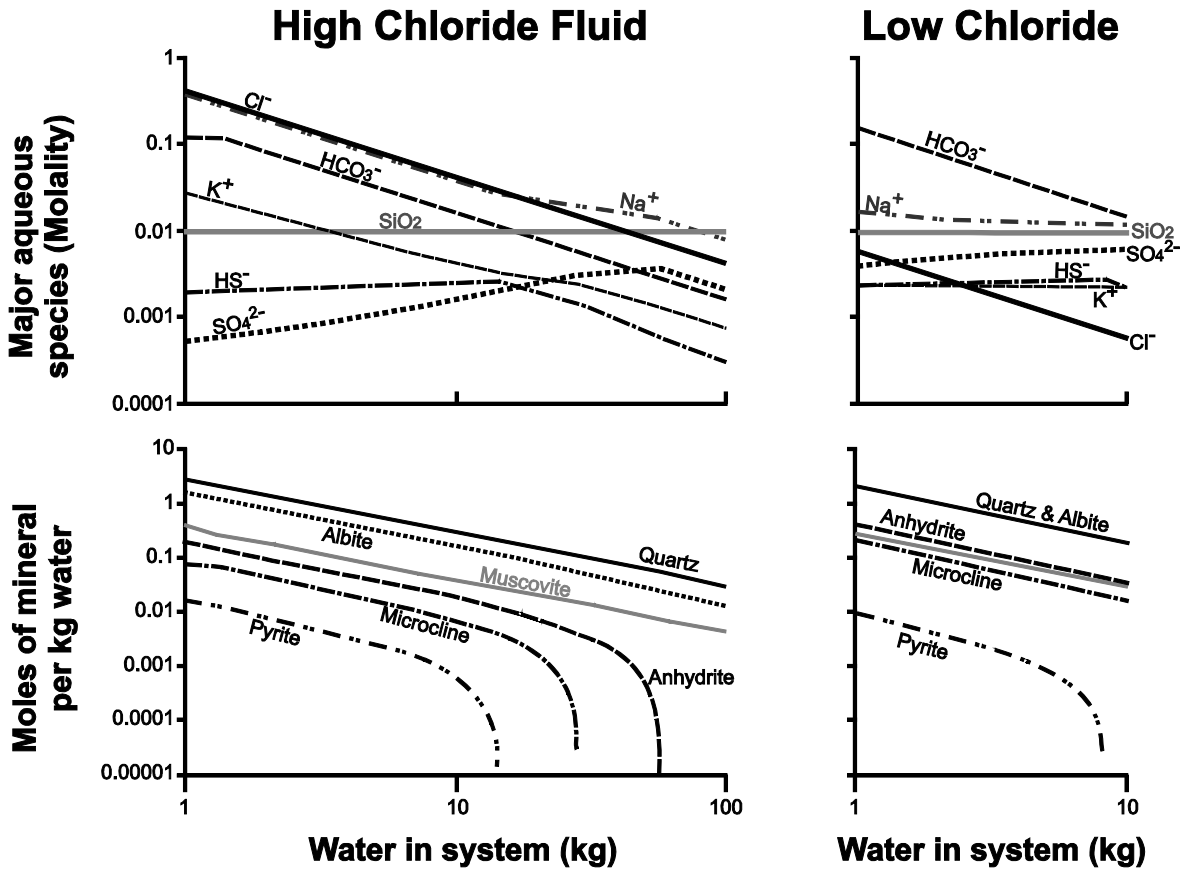

Fig. 9: Results of geochemical modelling showing effect of dilution on water chemistry. Secondary mineral assemblages buffer the dissolved species, and so aqueous silica and sulphate maintain or increase in concentration, whereas conservative species such as chloride are simply diluted. Upper plots show major dissolved components in molality, lower plots show major mineral phases present in alteration assemblage (normalised to total amount of water in system).